energies

Review

# Progress in Catalytic Hydrogen Production from Formic Acid over Supported Metal Complexes

**Dmitri A. Bulushev**

Laboratory of Catalytic Methods of Solar Energy Transformation, Boreskov Institute of Catalysis, SB RAS, 630090 Novosibirsk, Russia; dmitri.bulushev@catalysis.ru

**Abstract:** Formic acid is a liquid organic hydrogen carrier giving hydrogen on demand using catalysts. Metal complexes are known to be used as efficient catalysts for the hydrogen production from formic acid decomposition. Their performance could be better than those of supported catalysts with metal nanoparticles. However, difficulties to separate metal complexes from the reaction mixture limit their industrial applications. This problem can be resolved by supporting metal complexes on the surface of different supports, which may additionally provide some surface sites for the formic acid activation. The review analyzes the literature on the application of supported metal complexes in the hydrogen production from formic acid. It shows that the catalytic activity of some stable Ru and Ir supported metal complexes may exceed the activity of homogeneous metal complexes used for deposition. Non-noble metal-based complexes containing Fe demonstrated sufficiently high performance in the reaction; however, they can be poisoned by water present in formic acid. The proposed review could be useful for development of novel catalysts for the hydrogen production.

**Keywords:** formic acid decomposition; hydrogen; biomass; metal complex; heterogeneous catalyst; ruthenium; iridium; iron

check for updates

**Citation:** Bulushev, D.A. Progress in Catalytic Hydrogen Production from Formic Acid over Supported Metal Complexes. *Energies* **2021**, *14*, 1334. https://doi.org/10.3390/en14051334

Academic Editors: Ricardo Bessa and Wei-Hsin Chen

Received: 23 January 2021
Accepted: 22 February 2021
Published: 1 March 2021

## 1. Introduction

Hydrogen is mainly used for ammonia synthesis and the petrochemical industry. Its traditional production involves non-renewable sources and processes giving a significant emission of carbon dioxide leading to global warming. Among these processes are steam reforming of natural gas and gasification of coal performed at very high temperatures (>900 K). Recently, the International Energy Agency reported that the hydrogen production reached 75 mln of tons and that it was accompanied by emission of 830 mln tons of $CO_2$ [1]. Global demand for hydrogen increases from year to year accompanying by an increase of the carbon dioxide emissions.

Despite hydrogen is a clean energy carrier its safe transportation and storage are rather complicated. Liquid organic hydrogen carriers (LOHCs) are used for safe storage and transportation of hydrogen [2,3]. They can be produced from biomass or $CO_2$ thus avoiding the effect of the evolved $CO_2$ for global warming. Formic acid (HCOOH) is an example of such a LOHC. It contains 53.4 g $L^{-1}$ hydrogen (4.4 wt %), which is by a factor of 2 higher than the content of compressed hydrogen at 350 bar at the same volume. This amount corresponds to the energy density of 2.1 kWh $L^{-1}$. In contrast to hydrogen, formic acid can be easily transported and stored and its application is much safer. An important feature of using formic acid is that it can be produced by catalytic hydrolysis/oxidation of biomass with high yields at low temperatures (<423 K) [4–6]. Hydrogen can be released from formic acid using catalysts at even lower temperatures (Figure 1). Thus, transformation of biomass to hydrogen through formic acid could be considered as an efficient route, because direct gasification of biomass also giving hydrogen demands very high temperatures (>900 K) (Figure 1). Recently, Zhang et al. [7] and Park et al. [8] demonstrated the proof of concept for such an approach.

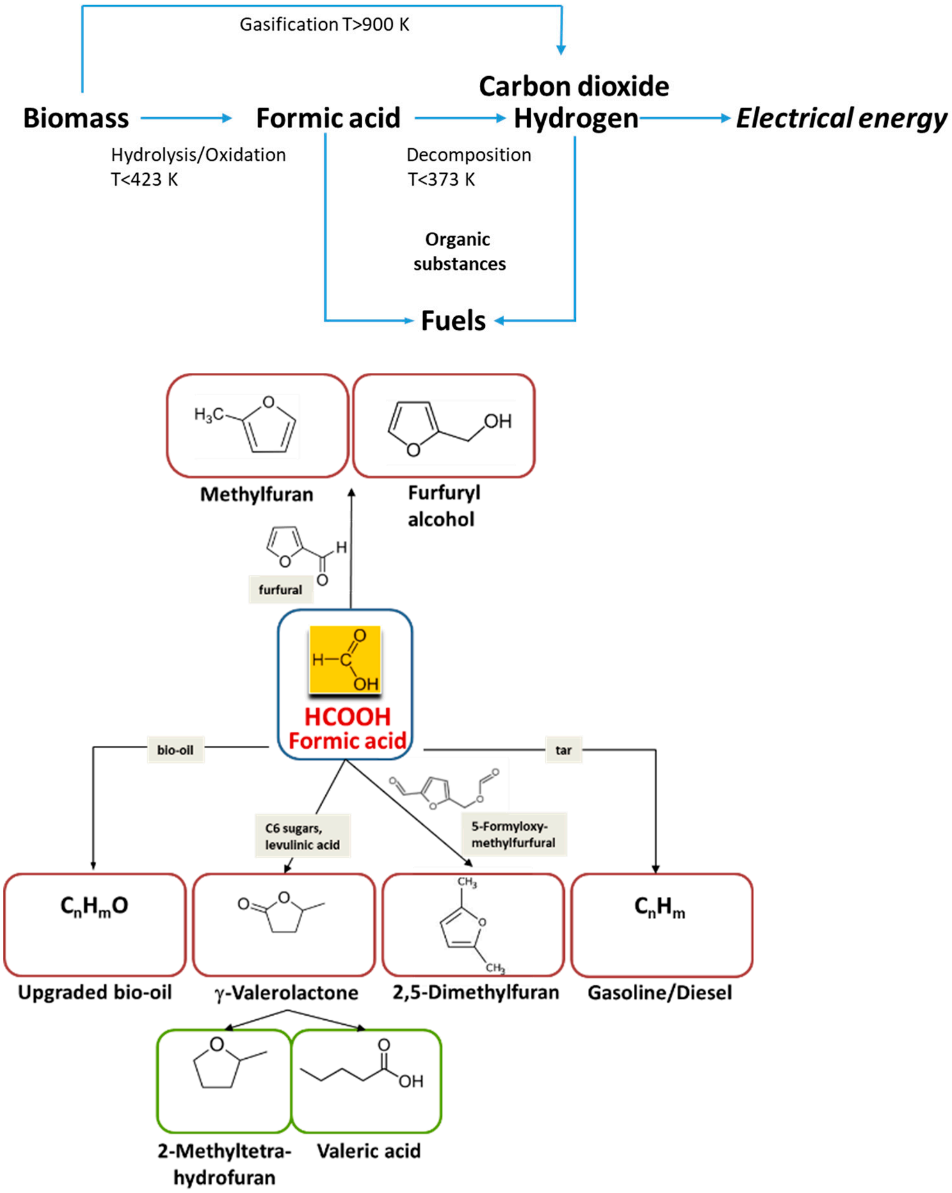

**Figure 1.** Reaction scheme showing the production of electrical energy and fuels from biomass through the conversion to formic acid.

The hydrogen obtained from formic acid could be further transformed to electrical energy (Figure 1). The development of a compact integrated 25 kW system which converts formic acid to power has been discussed [9]. Formic acid could be used also as a donor of hydrogen instead of molecular hydrogen to hydrogenate different organic substances for production of fuels and intermediates for fuels [4,10]. Thus, it could be applied for synthesis of γ-valerolactone from C6 sugars and levulinic acid [11], 2,5-dimethylfuran from 5-formyloxymethylfurfural [12], furfuryl alcohol [13] and methylfuran [14] from furfural, upgraded bio-oil from bio-oil [15], and diesel/gasoline mixtures from tar [16] (Figure 1).

Supported catalysts with nanoparticles are traditional catalysts for the hydrogen production from formic acid in gas and liquid phase. Novel single atom metal catalysts supported on N-doped carbon may provide a higher activity in the formic acid decomposition than the activity of the catalysts with nanoparticles, but the difference is not so significant [17]. The activity of homogeneous metal complexes is often higher [18–24]. Hence, they could be used at lower temperatures. Metal complexes also represent more uniform active sites as compared to metal nanoparticles. Hence, basing on this knowledge the design of the catalyst could be facilitated. However, there are serious problems of application of homogeneous metal complexes as catalysts for different reactions limiting their industrial applications. They include difficulties in separation of a catalyst from the reaction medium and catalyst's recovery, instability of homogeneous catalytic systems, as well as possible corrosive effects of catalyst solutions on the equipment [25].

Separation of the catalysts with noble metals could be important for production of hydrogen from reaction mixtures containing formic acid and obtained from biomass. To solve this problem, metal complexes could be supported on different supports. Serious efforts have been directed toward the immobilization of homogeneous catalysts on supports. Evidently, their catalytic properties could change due to a change of ligand environment, since after supporting the support surface sites become important ligands for metal atoms. These sites may have no direct analogs in solutions [25]. Their nature affects strongly the energy of interaction of metal complexes and resistance of the catalyst to leaching. Additionally, the support may provide surface sites for formic acid activation leading to its faster conversion.

Carbon dioxide is also produced as a by-product during the decomposition of formic acid; however, it can be further hydrogenated into formate salts at low temperatures [26,27]. Earlier, we have analyzed this reaction taking place on different catalysts, particularly on supported metal complexes [27]. In the present review, we will consider in details the catalytic properties of supported Ru, Ir and Fe complexes in the hydrogen production from formic acid. There are only a few studies performed with supported complexes of other metals (Pd, Rh) in this reaction. We have not found a specialized review related to application of supported metal complexes in the hydrogen production from formic acid. However, this subject is worth to discuss since this type of the catalysts shows excellent activity, selectivity and stability in the reaction and can be easily separated from the reaction mixture.

## 2. Supported Ruthenium Complexes

Ru complexes are among the most active complexes for the hydrogen production from liquid phase formic acid. The group of Laurenczy contributed significantly to the development of these catalysts [20]. In 2009, they reported the results of immobilization of ruthenium(II)–TPPTS (trisulfonated triphenylphosphine) complex on different supports [28]. Among them, they used an ion exchange resin containing basic trimethylammonium groups. The reaction mixture except of formic acid contained sodium formate (9:1). It is known that addition of sodium formate to formic acid should give a higher activity [19,29,30]. The results showed that this resin ionically interacted strongly with the Ru complex and no Ru leaching took place during the reaction. However, recycling of the catalyst led to a decrease in the reaction rate, but the same conversion was achieved in 3 h.

In another case, covalent interaction of the Ru species to the phosphine groups of $PPh_3$- or $PPh_3$-O-cross-linked polystyrene led to strong coordination of the metal. Unfortunately, the obtained catalyst was not sufficiently active in the reaction as compared to the homogeneous catalyst. The authors supposed that the reasons are related to a high hydrophobicity of the material and mass transfer limitations.

Additionally, they used five different types of zeolites as supports. The activity was sufficiently good, but the adsorbed Ru–TPPTS could be removed in water from zeolites thus indicating that it was attached weakly through physical adsorption. This complicates the catalyst recycling which is necessary for a sustainable process.

The same group has noticed later that their earlier attempts to create heterogenized metal complex catalysts were only partially successful and developed another system [29]. In this case, they used a mesoporous silica support (MCM-41) with attached phosphine groups. The optimized catalytic system corresponded to MCM41-Si-$(CH_2)_nPPh_2$/Ru-mTPPTS with $n = 2$ and demonstrated the activity and stability comparable to those of the homogeneous catalyst (Figure 2). Thus, the turnover frequency (TOF) of 2780 $h^{-1}$ was obtained at 383 K (Table 1). TOF value corresponds to the number of hydrogen molecules obtained per one metal site per time unit. It is a major value characterizing the specific activity of the catalysts.

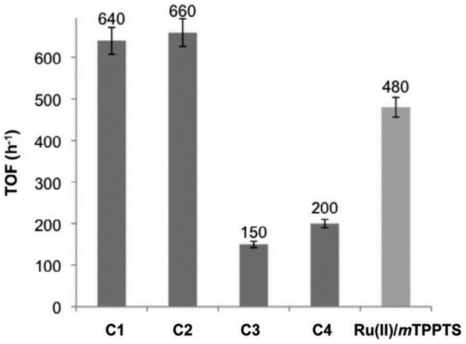

**Figure 2.** Effect of the number of $CH_2$ groups attaching phosphine groups to the MCM-41 support on formic acid (HCOOH) decomposition catalyzed by the immobilized Ru catalysts at 363 K. Reprinted with permission from [29].

The effect of the number of $CH_2$ groups attaching the phosphine groups ($n$) is demonstrated in Figure 2. It is seen that short $CH_2$ chains lead to the activity higher than those for the catalysts with longer chains. The content of CO obtained as a by-product was negligible (3 ppm). It is very important to have a very low level of CO in the reaction to prevent poisoning of the catalyst in a fuel cell. In addition, the supported Ru catalysts were recyclable since they allowed performing the reaction for more than 20 cycles without loss in activity.

Later, the same group created a reactor system for continuous production of hydrogen from formic acid [31]. A Ru-mTPPTS catalyst supported on phosphinated polystyrene beads was used in this case. This catalyst provided the TOF of 270 $h^{-1}$ at 378 K and the apparent activation energy of 93.6 kJ $mol^{-1}$. The low CO concentration level (<5 ppm) was reached due to a PROX reaction using a $Pt/CeO_2$ catalyst. Alternatively, a methanation of CO could be used to decrease the CO content [9].

Zhao [32] modified the surface of $SiO_2$ support (450 $m^2$ $g^{-1}$) with 3-mercaptopropyltrimethoxysilane to obtain $SiO_2$-SH groups, which then interacted with Ru or Pd chlorides (about 2 wt %). The obtained Ru-S-$SiO_2$ and Pd-S-$SiO_2$ catalysts showed TOFs of 344 $h^{-1}$ and 719 $h^{-1}$ with a 4 M HCOOH/HCOONa (9:1) mixture at 358 K, respectively. X-Ray Photoelectron Spectroscopy (XPS) studies before and after experiments showed the presence of mainly $Pd^{2+}$ ions in the catalyst indicating that they are the active sites of the reaction. The authors also showed that sulfates accelerate the reaction by up to 70%. This could be useful for practical applications.

Wang et al. [33] used a ruthenium pincer complex knitted in a porous organic polymer (810 $m^2$ $g^{-1}$). Thermal gravimetric analysis revealed that the supported complex was thermally stable up to 533 K. However, the TOF of 266 $h^{-1}$ obtained at 363 K was not very high. The authors proposed a mechanism for the formic acid decomposition and production based on participation of Ru hydride in the reaction (Figure 3). For the decomposition, the mechanism involves the dissociative formic acid adsorption and $CO_2$ release followed by $H_2$ release. It is interesting that N sites of the complex provide deprotonation of the formic acid through dissociation of the O–H bond.

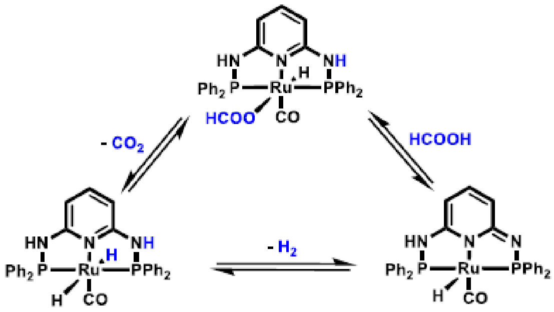

**Figure 3.** Proposed mechanism for the Ph-PN$_3$P Ru-catalyzed formic acid dehydrogenation and CO$_2$ hydrogenation. Reprinted with permission from [33].

Solakidou et al. [34] showed that amino functionalized silica ($H_2N@SiO_2$) significantly increases the TOFs of the hydrogen production from formic acid by a ($Ru/P(CH_2CH_2PPh_2)_3$) homogeneous catalyst. The maximal TOF reached 983 $h^{-1}$ at 363 K. They observed a significant decrease of the apparent activation energy from 41 kJ $mol^{-1}$ to 28 kJ $mol^{-1}$ and supposed that the $H_2N@SiO_2$ particles play a dual role: they act as a co-catalyst for deprotonating formic acid by amine groups, and they serve as a template, which stabilizes the metal complex on its surface, thus promoting formate decomposition via ($Ru^{II}$-hydride) species.

Bavykina et al. [35] used a Ru complex supported on covalent triazine framework ($Ru^{II}(\eta_6\text{-}C_6H_6)$/CTF) and obtained high TOF values at 353 K in base free conditions (without Na formate) (4020 $h^{-1}$, Table 1).

Hausoul et al. [36] studied the effect of the nature of polymeric support on the properties of a Ru complex in the hydrogen production from formic acid. Polymeric analogs of $PPh_3$ (pTPP), 1,2-bis(diphenylphosphino)ethane (pDPPE) (Figure 4), and 1,2-(diphenylphosphino)benzene (pDPPBe) have been tested. The highest TOF of 22,900 $h^{-1}$ was obtained with a $RuCl_2$(p-cymene)/pDPPE catalyst at 433 K (Table 1). The catalyst performed efficiently in solutions with up to 30 wt % formic acid. It is seen in Figure 5a that the activity of the unsupported ($RuCl_2$(p-cymene)($PPh_3$)) complex is significantly lower than those of the supported complexes. The kinetics of the reaction was featured by an induction period and a pseudo-zero-order dynamics of the pressure increase. Recycling experiments revealed only low leaching and a small decrease in the activity over 7 runs. A Ru/C catalyst with nanoparticles gave a significantly lower activity, lower selectivity and leaching of Ru to the reaction solution.

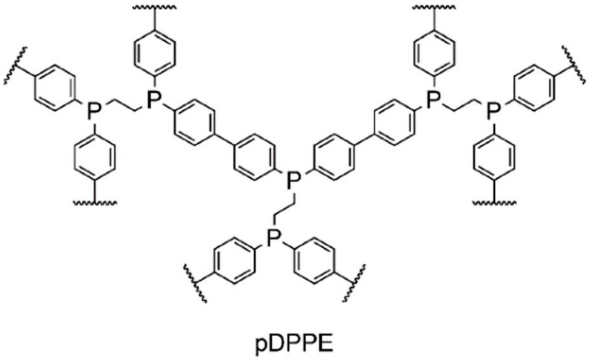

**Figure 4.** pDPPE.

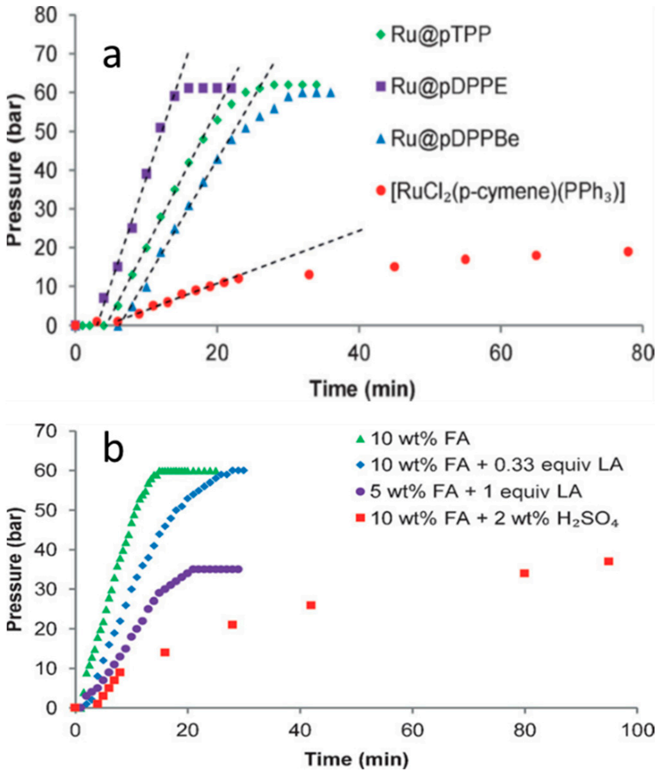

**Figure 5.** (**a**) Reactor pressure in the Ru-catalyzed decomposition of aqueous formic acid at 433 K. (**b**) Effect of admixtures on decomposition of formic acid on the Ru@pDPPE catalyst. Reprinted with permission from [36].

The same authors studied the decomposition of formic acid in solutions with other substances (Figure 5b). It is seen that levulinic acid (LA) and sulfuric acid retard the reaction, but they do not poison the catalyst completely. This is important to know for development of future biorefineries involving the process of conversion of biomass to hydrogen through the formic acid production [7,8] (Figure 1).

Beloqui Redondo et al. [37] used a 0.4 wt % Ru phosphine complex supported on a metal organic framework (MOF) for the gas phase decomposition of formic acid at 418 K. They obtained 99% selectivity and TOF of 2300 $h^{-1}$ (Table 1). This TOF is sufficiently high for the gas phase decomposition. The authors indicated that phosphine species interact with Ru species providing the formation of Ru single-sites on the MOF support. Amine linkers present in the support could activate formic acid for the reaction through deprotonation. The authors observed an induction period, which was assigned to removal of chloride ligands from the metal complex followed by coordination of formates. However, the Brunauer–Emmett–Teller (BET) surface area of their catalyst decreased significantly after the reaction. It is not clear whether this will take place further and affect negatively the catalytic reaction.

## 3. Supported Iridium Complexes

As we showed above, several Ru complexes, which are very active in the formic acid decomposition, involve phosphine ligands. Broicher et al. [38] indicated that P-based ligands are sensitive to oxidation, while N-based ligands show a great advantage allowing handling and storage of the catalyst in air. In this section, we will consider Ir complexes, which are mainly attached to N-containing ligands of the support.

Bavykina et al. [35] have used an [IrCp*(OH)](OTf)$_2$ complex (OTf-triflate) to deposit over a covalent triazine framework (CTF) prepared at 773 K with a high surface area (Figure 6a,b). OTf was washed out during the recycling of the catalyst, pointing that formate replaces triflate. The TOFs of the catalysts with a low concentration of the metal complex (0.2 wt %) were higher than those of the catalysts with a high concentration and corresponded to 27,000 $h^{-1}$ (Table 1).

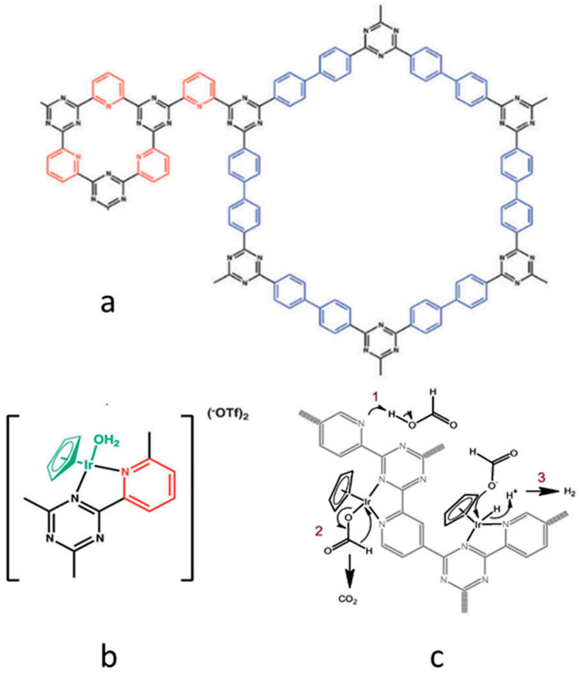

**Figure 6.** (**a**) Covalent triazine framework (CTF) support unit, (**b**) $[IrCp^*(OH)](OTf)_2$ complex attached to the CTF support, and (**c**) scheme showing a catalytic cycle within the CTF support involving the steps of (1) formic acid interaction, (2) β-hydride elimination, and (3) hydrogen release. Adapted with permission from [35].

The authors tested the catalyst's durability in continuous mode. Thus, a highly concentrated formic acid solution (88 wt %) was fed to a reactor at 353 K. At termination of this experiment, a turnover number (TON = the number of $H_2$ molecules related to the number of metal sites) of 1,060,000 was obtained, which demonstrates that the catalyst is highly durable and can be used in devices producing hydrogen.

Figure 6c displays possible molecular pathways for the system [35], which consist of the three main steps: (1) formic acid deprotonation, (2) β-hydride elimination and (3) hydrogen release. The deprotonation is important and takes place on free pyridinic sites that provide basicity of the CTF support. The hydrogen release step has been proposed to be rate-determining.

Gunasekar et al. [39] studied an $[IrCp^*Cl_2]_2$ complex supported on CTFs prepared at different temperatures 673 and 773 K. The activity of the supported complex was higher than that of the homogeneous complex. The TOFs were, however, lower than those obtained by Bavykina et al. [35] and corresponded to 7930 $h^{-1}$ at 363 K. This could be related to a much higher concentration of metal in the samples. The TOF for the similar supported RhCp* complex was lower than that of the IrCp* complex.

Shen et al. [30] studied an $IrCp^*Cl_2$ complex supported on porous polypyrrole particles (500 nm) with a BET surface area of 51 $m^2$ $g^{-1}$ (Table 1). The TOF was very high in the presence of sodium formate and equal to 46,000 $h^{-1}$ at 363 K. The apparent activation energy in the formic acid decomposition in the absence of sodium formate corresponded to 63 kJ $mol^{-1}$ and in the presence of sodium formate it was approximately the same (66 kJ $mol^{-1}$). When 1.0 M formic acid solution flowed into a tubular reactor (55 × 9 mm) with a catalyst containing 250 mg of the $IrCp^*Cl_2$(polypyrolle) complex at 313 K, the initial hydrogen evolving rate was 5.6 mL $min^{-1}$, which could generate about 1.1 W electric power through a proton-exchange membrane fuel cell. The authors noted that this value was sufficient to drive, for example, a personal mobile phone.

Recently, Broicher et al. [38] also used an $[IrCp^*Cl_2]_2$ complex as a precatalyst and a conjugated microporous polymer (CMP) with bipyridine groups as a support. The combination of those gave an Ir@CMP catalyst (Figure 7). This catalyst showed a record value of TOF of 123,894 $h^{-1}$ at 433 K (Table 1), relatively high apparent activation barrier of 90 kJ $mol^{-1}$ and low leaching. The CO content was stable in the range around 68 ppm. Complete conversion of formic acid could be reached.

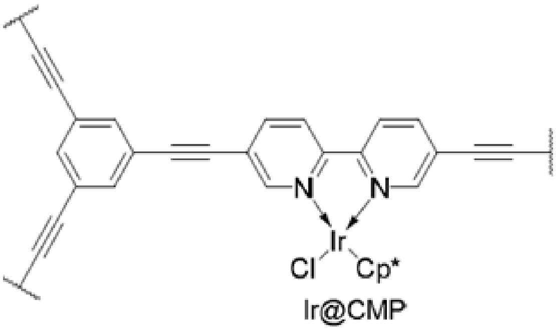

**Figure 7.** Ir@CMP catalyst.

In the same conditions a commercial Ir/C catalyst with nanoparticles demonstrated a strong leaching and gave a low conversion of formic acid confirming that Ir nanoparticles are not active in the reaction. Application of the $[IrCp^*Cl_2]_2$ complex without bipyridine ligands as a catalyst gave also only a low conversion. At the same time, the $[IrCp^*Cl_2/2,2\text{-bipy}]$ complex showed a high activity of 43,051 $h^{-1}$ at 433 K demonstrating the need for bipyridine ligands. The activity of the supported 1 wt % Ir@CMP catalyst (Figure 8) was close (35,246 $h^{-1}$) indicating that the heterogenization affected only weakly. After the reaction, a significant amount of nanoparticles (up to 5 nm) was found in the sample, demonstrating that the measured activity is really caused by a low number of active sites with a very high activity. This point is also supported by a study of the effect of variation of metal loading showing that the TOFs are higher for the catalysts with a low content of metal complex (Figure 8) in accordance with the data of Bavykina et al. [35].

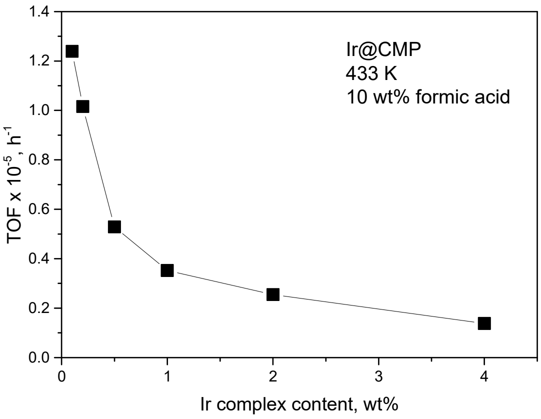

**Figure 8.** Effect of concentration of IrCp* complex supported on bipyridine-based conjugated microporous polymer on the TOFs in formic acid decomposition. The data are taken with permission from Reference [38].

## 4. Supported Iron Complexes

The use of efficient non-noble metal catalysts would be a good choice for the hydrogen production from formic acid decomposition. Boddien et al. [40] proposed different homogeneous Fe containing complexes for this reaction. Using a mixture of 0.005 mol% $Fe(BF_4)_2 \cdot 6H_2O$ and tris[(2-diphenylphosphino)ethyl]phosphine $[P(CH_2CH_2PPh_2)_3]$ to a solution of formic acid in propylene carbonate, without other additives or bases, obtained a

TOF value up to 9425 $h^{-1}$ and a TON value of more than 92,000 at 353 K [40]. The apparent activation energy corresponded to 77 kJ $mol^{-1}$ and the CO content did not exceed 20 ppm. However, the catalyst was completely poisoned and became inactive after 16 h of the continuous reaction. This was assigned to chloride and/or water admixtures accumulation on the catalyst.

Later, Stathi et al. [41] successfully heterogenized Fe phosphine complexes on the surface of two types of silica modified with phosphines (Figure 9a). Heterogenization of the Fe(II)/$P(CH_2CH_2PPh_2)_3$ system increased its TOF by 1.7 times as compared to the homogeneous catalyst and was in the range of 6000–8000 $h^{-1}$ (Table 1). The reaction was performed in propylene carbonate solvent. The apparent activation energies were significantly lower than that of the homogeneous complex and corresponded to 51 kJ $mol^{-1}$ and 43 kJ $mol^{-1}$ for $Fe^{II}/RPPh_2@SiO_2$ and $Fe^{II}$/polyRPhphos@$SiO_2$, respectively. The authors indicated that the possible rate determining steps could be hydride elimination or direct hydride transfer from formate to Fe. No leaching of iron in the reaction solution was found. The $Fe^{II}/RPPh_2@SiO_2$ catalyst showed a TON of higher than 176,000.

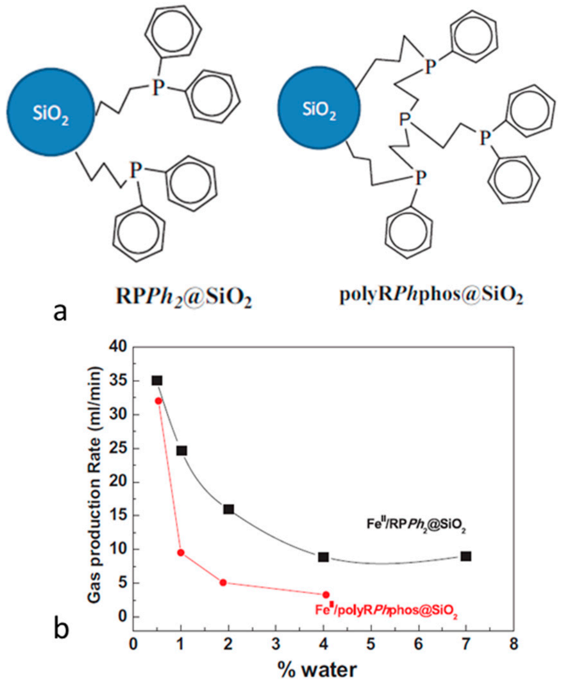

**Figure 9.** (**a**) Silica supports modified with phosphines. (**b**) Effect of water addition on the formic acid decomposition over supported Fe containing catalysts at 373 K. Reprinted with permission from [41].

The authors observed an inhibitory water effect (Figure 9b), but it was reversible, since the catalyst could be reactivated by a simple washing. This result is important to know, since formic acid always contains a small amount of water, which can be formed together with carbon monoxide due to self-decomposition of formic acid taking place during its storage [42]. This effect is more significant at high concentrations of formic acid.

**Table 1.** Properties of the most active supported Ru, Ir and Fe complexes used for the hydrogen production from formic acid.

| Initial or Attached Complex | Catalyst Support | BET Surface Area of the Support, $m^2\ g^{-1}$ | Active Metal Concentration, wt % | T, K | Concentration of Formic Acid and Sodium Formate | TOF, $h^{-1}$ (Ea, kJ $mol^{-1}$) | Reference |
|---|---|---|---|---|---|---|---|
| Ru-mTPPTS | MCM41-Si$(CH_2)_2PPh_2$ | - | 0.3 | 383 | 10 M (HCOOH+HCOONa, 9:1) | 2780 | [28] |
| $Ru^{II}(\eta_6-C_6H_6)$ | CTF500 | 1800 | 2.7 | 353 | 3 M | 4020 | [35] |
| $RuCl_2$(p-cymene) | pDPPE | 33 | 1 | 433 | 2.2 M | 22,900 | [36] |
| $RuCl_2$(p-cymene) | $PPh_2$-MOF | 1075 to 161 (after reaction) | 0.7 | 418 | 5 vol% (gas phase reaction) | 2300 | [37] |
| $Ir^{III}Cp^*$ | CTF500 | 1800 | 0.2 | 353 | 3 M | 27,000 | [35] |
| $[Cp^*IrCl_2]_2$ | bpy-CTF400 | 684 | 1.4 | 353 | 1 M | 2820 | [39] |
| $[Cp^*IrCl_2]_2$ | bpy-CTF500 | 1566 | 11.3 | 363 | 1 M | 7930 | [39] |
| $Cp^*IrCl_2$ | polypyrrole | 51 | 4.3 | 333 | 1 M | 4060 | [30] |
| $Cp^*IrCl_2$ | polypyrrole | 51 | 4.3 | 363 | 2 M (HCOOH+HCOONa,1:1) | 46,000 (66) | [30] |
| $[Cp^*IrCl_2]_2$ | CMP | 706 | 0.1 | 433 | 2.2 M | 123,894 (90) | [38] |
| $Fe(BF_4)_2$ | polyRPhphos@$SiO_2$ | 502 | 0.8 | 363 | 7.6 M | 7600 (51) | [41] |
| $Fe(BF_4)_2$ | $RPPh_2$@$SiO_2$ | 531 | 0.9 | 363 | 7.6 M | 6396 (43) | [41] |

Ea—apparent activation energy, mTPPTS—meta-trisulfonated triphenylphosphine, PPh—phenylphosphine, CTF—covalent triazine framework, MOF—metal organic framework, Cp*—pentamethylcyclopentadienyl, CMP—bipyridine-based conjugated microporous polymer.

## 5. Discussion

The summarized data for the key catalysts with supported Ru, Ir and Fe complexes for the hydrogen production from formic acid are shown in Table 1. Other metal complexes are almost not studied. The table can help to choose the optimal catalysts corresponding to certain conditions of the reaction. However, it is not easy to compare the activity of the catalysts (TOFs) presented in Table 1, since the conditions of the reaction and concentrations of the active component in the catalysts were different. Moreover, some experiments have been performed in the presence of sodium formate. Basic additives to the reaction mixture or basic sites of the catalysts/supports are known to promote significantly the reaction. They deprotonate formic acid to formate species. Deprotonation of formic acid can be provided also by traditional oxide supports having basic sites [43] and by introduction of alkali metals promoters to supported metal catalysts [44–46]. Deprotonation provided by pyridinic N sites of N-doped carbon support was also reported for the catalysts with single metal atoms [47,48]. In this case, it reminds the effect of basic amine additives.

As for catalysts with nanoparticles, the steady-state TOF values obtained for the gas-phase reaction over a Pd/C catalyst doped with K ions with 3–4 nm Pd nanoparticles did not exceed 3600 $h^{-1}$ at 353 K [44,45]. For the liquid-phase reaction and Pd nanoparticles (~1.4 nm) supported on N-doped carbon, the initial values were higher and reached 8414 $h^{-1}$ at 333 K in the presence of sodium formate [22]. Some supported catalysts with nanoparticles (Ir/C [38] and Ru/C [36]) were used for comparison of the activity with supported metal complexes (Table 1). It was shown that their activity is negligible as compared with the activity of supported metal complexes. The disadvantage of these comparisons was that the mean sizes of nanoparticles in the catalysts with nanoparticles were not reported.

In contrast, some homogeneous complexes showed much higher TOFs than those of the supported metal complexes (Table 1). The values in the range 250,000–322,000 $h^{-1}$ for temperatures 363 and 373 K have been reported by a few groups of authors [21,23,24]. These complexes are also based on Ir [23,24] and Ru [21]. It would be useful to immobilize them on some supports in order to have an opportunity to separate easily the obtained catalyst from the reaction mixture.

As it is shown above (Figure 8), concentration of a metal complex is an important factor determining TOFs. Interesting that at a lower concentration of a metal complex higher TOFs were observed. In this case, the active sites could be stabilized by specific support sites. The nature of these active sites should be studied using advanced methods like extended X-ray absorption fine structure (EXAFS) combined with X-ray absorption near edge structure (XANES) preferably in situ. Using density functional theory (DFT) calculations may assist in understanding the structure of these active sites. There is an evident lack of such studies. The progress in understanding may lead to development of a targeted synthesis of the catalysts with these very active sites.

## 6. Conclusions

Therefore, the analysis of the literature showed that immobilization of Ru, Ir and Fe complexes on some polymers, covalent triazine frameworks, metal organic frameworks or silica modified with phosphines is promising for the hydrogen production from formic acid in terms of activity of the catalysts and possibility to separate the catalysts from the reaction mixture. Supported Ir complexes were normally more efficient than the supported Ru complexes. Thus, the maximal TOF value was reached for the IrCp* complex supported on the bipyridine-based conjugated microporous polymer and corresponded to 123,894 $h^{-1}$ at 433 K. In part, the high activity of Ir complexes could be provided by the presence of basic N sites of the supports which deprotonate formic acid for further easier decomposition of the formed formate species with participation of the Ir atoms. Yet, the activities of some homogeneous metal complexes were higher and reached 322,000 $h^{-1}$.

A strong concentration effect of metal complexes was observed demonstrating that at a small concentration of supported metal complex higher TOFs are obtained than those at a high concentration. This effect is not related to nanoparticles formation. Finally, non-noble metal supported Fe complexes were efficient in the reaction provided the contents of water and chlorine ions in the solution were negligible.

**Funding:** The work was funded by the Russian Science Foundation (grant 17-73-30032).

**Institutional Review Board Statement:** Not applicable.

**Informed Consent Statement:** Not applicable.

**Data Availability Statement:** Data is contained within the article.

**Conflicts of Interest:** The authors declare no conflict of interest.

## References

1. IEA. The Future of Hydrogen. Available online: www.iea.org/reports/the-future-of-hydrogen (accessed on 26 February 2021).
2. Preuster, P.; Papp, C.; Wasserscheid, P. Liquid Organic Hydrogen Carriers (LOHCs): Toward a Hydrogen-free Hydrogen Economy. *Acc. Chem. Res.* **2017**, *50*, 74–85. [CrossRef] [PubMed]
3. Rao, P.C.; Yoon, M. Potential Liquid-Organic Hydrogen Carrier (LOHC) Systems: A Review on Recent Progress. *Energies* **2020**, *13*, 6040. [CrossRef]
4. Bulushev, D.A.; Ross, J.R.H. Towards Sustainable Production of Formic Acid. *ChemSusChem* **2018**, *11*, 821–836. [CrossRef]
5. Gromov, N.V.; Medvedeva, T.B.; Rodikova, Y.A.; Babushkin, D.E.; Panchenko, V.N.; Timofeeva, M.N.; Zhizhina, E.G.; Taran, O.P.; Parmon, V.N. One-pot synthesis of formic acid via hydrolysis–oxidation of potato starch in the presence of cesium salts of heteropoly acid catalysts. *RSC Adv.* **2020**, *10*, 28856–28864. [CrossRef]
6. Preuster, P.; Albert, J. Biogenic Formic Acid as a Green Hydrogen Carrier. *Energy Technol.* **2018**, *6*, 501–509. [CrossRef]
7. Zhang, P.; Guo, Y.-J.; Chen, J.; Zhao, Y.-R.; Chang, J.; Junge, H.; Beller, M.; Li, Y. Streamlined hydrogen production from biomass. *Nat. Catal.* **2018**, *1*, 332–338. [CrossRef]
8. Park, J.-H.; Lee, D.-W.; Jin, M.-H.; Lee, Y.-J.; Song, G.-S.; Park, S.-J.; Jung, H.J.; Oh, K.K.; Choi, Y.-C. Biomass-formic acid-hydrogen conversion process with improved sustainability and formic acid yield: Combination of citric acid and mechanocatalytic depolymerization. *Chem. Eng. J.* **2020**, 127827. [CrossRef]
9. Van Putten, R.; Wissink, T.; Swinkels, T.; Pidko, E.A. Fuelling the hydrogen economy: Scale-up of an integrated formic acid-to-power system. *Int. J. Hydrogen Energy* **2019**, *44*, 28533–28541. [CrossRef]
10. Nie, R.; Tao, Y.; Nie, Y.; Lu, T.; Wang, J.; Zhang, Y.; Lu, X.; Xu, C.C. Recent Advances in Catalytic Transfer Hydrogenation with Formic Acid over Heterogeneous Transition Metal Catalysts. *ACS Catal.* **2021**, *11*, 1071–1095. [CrossRef]
11. Heeres, H.; Handana, R.; Chunai, D.; Borromeus Rasrendra, C.; Girisuta, B.; Jan Heeres, H. Combined dehydration/(transfer)-hydrogenation of C6-sugars (D-glucose and D-fructose) to $\gamma$-valerolactone using ruthenium catalysts. *Green Chem.* **2009**, *11*, 1247–1255. [CrossRef]
12. Sun, Y.; Xiong, C.; Liu, Q.; Zhang, J.; Tang, X.; Zeng, X.; Liu, S.; Lin, L. Catalytic Transfer Hydrogenolysis/Hydrogenation of Biomass-Derived 5-Formyloxymethylfurfural to 2, 5-Dimethylfuran Over Ni–Cu Bimetallic Catalyst with Formic Acid As a Hydrogen Donor. *Ind. Eng. Chem. Res.* **2019**, *58*, 5414–5422. [CrossRef]
13. Nagaiah, P.; Gidyonu, P.; Ashokraju, M.; Rao, M.V.; Challa, P.; Burri, D.R.; Kamaraju, S.R.R. Magnesium Aluminate Supported Cu Catalyst for Selective Transfer Hydrogenation of Biomass Derived Furfural to Furfuryl Alcohol with Formic Acid as Hydrogen Donor. *ChemistrySelect* **2019**, *4*, 145–151. [CrossRef]
14. Fu, Z.; Wang, Z.; Lin, W.; Song, W.; Li, S. High efficient conversion of furfural to 2-methylfuran over Ni-Cu/$Al_2O_3$ catalyst with formic acid as a hydrogen donor. *Appl. Catal. A Gen.* **2017**, *547*, 248–255. [CrossRef]
15. Bulushev, D.A.; Ross, J.R.H. Catalysis for conversion of biomass to fuels via pyrolysis and gasification: A review. *Catal. Today* **2011**, *171*, 1–13. [CrossRef]
16. Chesnokov, V.V.; Dik, P.P.; Chichkan, A.S. Formic Acid as a Hydrogen Donor for Catalytic Transformations of Tar. *Energies* **2020**, *13*, 4515. [CrossRef]
17. Bulushev, D.A.; Bulusheva, L.G. Catalysts with single metal atoms for the hydrogen production from formic acid. *Catal. Rev.* **2021**, 1–40. [CrossRef]
18. Li, Z.; Xu, Q. Metal-Nanoparticle-Catalyzed Hydrogen Generation from Formic Acid. *Acc. Chem. Res.* **2017**, *50*, 1449–1458. [CrossRef]
19. Stathi, P.; Solakidou, M.; Louloudi, M.; Deligiannakis, Y. From Homogeneous to Heterogenized Molecular Catalysts for $H_2$ Production by Formic Acid Dehydrogenation: Mechanistic Aspects, Role of Additives, and Co-Catalysts. *Energies* **2020**, *13*, 733. [CrossRef]
20. Laurenczy, G.; Dyson, P.J. Homogeneous Catalytic Dehydrogenation of Formic Acid: Progress Towards a Hydrogen-Based Economy. *J. Braz. Chem. Soc.* **2014**, *25*, 2157–2163. [CrossRef]
21. Filonenko, G.A.; van Putten, R.; Schulpen, E.N.; Hensen, E.J.M.; Pidko, E.A. Highly Efficient Reversible Hydrogenation of Carbon Dioxide to Formates Using a Ruthenium PNP-Pincer Catalyst. *ChemCatChem* **2014**, *6*, 1526–1530. [CrossRef]

22. Onishi, N.; Iguchi, M.; Yang, X.; Kanega, R.; Kawanami, H.; Xu, Q.; Himeda, Y. Development of Effective Catalysts for Hydrogen Storage Technology Using Formic Acid. *Adv. Energy Mater.* **2019**, *9*, 1801275. [CrossRef]
23. Papp, G.; Ölveti, G.; Horváth, H.; Kathó, Á.; Joó, F. Highly efficient dehydrogenation of formic acid in aqueous solution catalysed by an easily available water-soluble iridium(iii) dihydride. *Dalton Trans.* **2016**, *45*, 14516–14519. [CrossRef] [PubMed]
24. Wang, W.-H.; Ertem, M.Z.; Xu, S.; Onishi, N.; Manaka, Y.; Suna, Y.; Kambayashi, H.; Muckerman, J.T.; Fujita, E.; Himeda, Y. Highly Robust Hydrogen Generation by Bioinspired Ir Complexes for Dehydrogenation of Formic Acid in Water: Experimental and Theoretical Mechanistic Investigations at Different pH. *ACS Catal.* **2015**, *5*, 5496–5504. [CrossRef]
25. Yermakov, Y.I.; Kuznetsov, B.N.; Zakharov, V.A. Chapter 1: Introduction to the Field of Catalysis by Supported Complexes. In *Studies in Surface Science and Catalysis*; Elsevier: Amsterdam, The Netherlands, 1981; Volume 8, pp. 1–58. [CrossRef]
26. Álvarez, A.; Bansode, A.; Urakawa, A.; Bavykina, A.V.; Wezendonk, T.A.; Makkee, M.; Gascon, J.; Kapteijn, F. Challenges in the Greener Production of Formates/Formic Acid, Methanol, and DME by Heterogeneously Catalyzed $CO_2$ Hydrogenation Processes. *Chem. Rev.* **2017**, *117*, 9804–9838. [CrossRef]
27. Bulushev, D.A.; Ross, J.R.H. Heterogeneous catalysts for hydrogenation of $CO_2$ and bicarbonates to formic acid and formates. *Catal. Rev.* **2018**, *60*, 566–593. [CrossRef]
28. Gan, W.; Dyson, P.J.; Laurenczy, G. Hydrogen storage and delivery: Immobilization of a highly active homogeneous catalyst for the decomposition of formic acid to hydrogen and carbon dioxide. *React. Kinet. Catal. Lett.* **2009**, *98*, 205. [CrossRef]
29. Gan, W.; Dyson, P.J.; Laurenczy, G. Heterogeneous Silica-Supported Ruthenium Phosphine Catalysts for Selective Formic Acid Decomposition. *ChemCatChem* **2013**, *5*, 3124–3130. [CrossRef]
30. Shen, Y.; Zhan, Y.; Bai, C.; Ning, F.; Wang, H.; Wei, J.; Lv, G.; Zhou, X. Immobilized iridium complexes for hydrogen evolution from formic acid dehydrogenation. *Sustain. Energy Fuels* **2020**, *4*, 2519–2526. [CrossRef]
31. Yuranov, I.; Autissier, N.; Sordakis, K.; Dalebrook, A.F.; Grasemann, M.; Orava, V.; Cendula, P.; Gubler, L.; Laurenczy, G. Heterogeneous Catalytic Reactor for Hydrogen Production from Formic Acid and Its Use in Polymer Electrolyte Fuel Cells. *ACS Sustain. Chem. Eng.* **2018**, *6*, 6635–6643. [CrossRef]
32. Zhao, Y.; Deng, L.; Tang, S.-Y.; Lai, D.-M.; Liao, B.; Fu, Y.; Guo, Q.-X. Selective Decomposition of Formic Acid over Immobilized Catalysts. *Energy Fuels* **2011**, *25*, 3693–3697. [CrossRef]
33. Wang, X.; Ling, E.A.P.; Guan, C.; Zhang, Q.; Wu, W.; Liu, P.; Zheng, N.; Zhang, D.; Lopatin, S.; Lai, Z.; et al. Single-Site Ruthenium Pincer Complex Knitted into Porous Organic Polymers for Dehydrogenation of Formic Acid. *ChemSusChem* **2018**, *11*, 3591–3598. [CrossRef]
34. Solakidou, M.; Deligiannakis, Y.; Louloudi, M. Heterogeneous amino-functionalized particles boost hydrogen production from Formic Acid by a ruthenium complex. *Int. J. Hydrogen Energy* **2018**, *43*, 21386–21397. [CrossRef]
35. Bavykina, A.V.; Goesten, M.G.; Kapteijn, F.; Makkee, M.; Gascon, J. Efficient production of hydrogen from formic acid using a Covalent Triazine Framework supported molecular catalyst. *ChemSusChem* **2015**, *8*, 809–812. [CrossRef]
36. Hausoul, P.J.C.; Broicher, C.; Vegliante, R.; Göb, C.; Palkovits, R. Solid Molecular Phosphine Catalysts for Formic Acid Decomposition in the Biorefinery. *Angew. Chem. Int. Ed.* **2016**, *55*, 5597–5601. [CrossRef]
37. Beloqui Redondo, A.; Morel, F.L.; Ranocchiari, M.; van Bokhoven, J.A. Functionalized Ruthenium–Phosphine Metal–Organic Framework for Continuous Vapor-Phase Dehydrogenation of Formic Acid. *ACS Catal.* **2015**, *5*, 7099–7103. [CrossRef]
38. Broicher, C.; Foit, S.R.; Rose, M.; Hausoul, P.J.C.; Palkovits, R. A Bipyridine-Based Conjugated Microporous Polymer for the Ir-Catalyzed Dehydrogenation of Formic Acid. *ACS Catal.* **2017**, *7*, 8413–8419. [CrossRef]
39. Gunasekar, G.H.; Kim, H.; Yoon, S. Dehydrogenation of formic acid using molecular Rh and Ir catalysts immobilized on bipyridine-based covalent triazine frameworks. *Sustain. Energy Fuels* **2019**, *3*, 1042–1047. [CrossRef]
40. Boddien, A.; Mellmann, D.; Gärtner, F.; Jackstell, R.; Junge, H.; Dyson, P.J.; Laurenczy, G.; Ludwig, R.; Beller, M. Efficient Dehydrogenation of Formic Acid Using an Iron Catalyst. *Science* **2011**, *333*, 1733. [CrossRef] [PubMed]
41. Stathi, P.; Deligiannakis, Y.; Avgouropoulos, G.; Louloudi, M. Efficient $H_2$ production from formic acid by a supported iron catalyst on silica. *Appl. Catal. A Gen.* **2015**, *498*, 176–184. [CrossRef]
42. Hietala, J.; Vuori, A.; Johnsson, P.; Pollari, I.; Reutemann, W.; Kieczka, H. Formic Acid. In *Ullmann's Encyclopedia of Industrial Chemistry*; Wiley-VCH Verlag GmbH & Co. KGaA: Weinheim, Germany, 2016; pp. 1–22. [CrossRef]
43. Zacharska, M.; Chuvilin, A.L.; Kriventsov, V.V.; Beloshapkin, S.; Estrada, M.; Simakov, A.; Bulushev, D.A. Support effect for nanosized Au catalysts in hydrogen production from formic acid decomposition. *Catal. Sci. Technol.* **2016**, *6*, 6853–6860. [CrossRef]
44. Jia, L.; Bulushev, D.A.; Beloshapkin, S.; Ross, J.R.H. Hydrogen production from formic acid vapour over a Pd/C catalyst promoted by potassium salts: Evidence for participation of buffer-like solution in the pores of the catalyst. *Appl. Catal. B-Environ.* **2014**, *160*, 35–43. [CrossRef]
45. Jia, L.; Bulushev, D.A.; Ross, J.R.H. Formic acid decomposition over palladium based catalysts doped by potassium carbonate. *Catal. Today* **2016**, *259*, 453–459. [CrossRef]
46. Bulushev, D.A.; Zacharska, M.; Guo, Y.; Beloshapkin, S.; Simakov, A. CO-free hydrogen production from decomposition of formic acid over Au/$Al_2O_3$ catalysts doped with potassium ions. *Catal. Commun.* **2017**, *92*, 86–89. [CrossRef]

47. Bing, Q.M.; Liu, W.; Yi, W.C.; Liu, J.Y. Ni anchored $C_2N$ monolayers as low-cost and efficient catalysts for hydrogen production from formic acid. *J. Power Sources* **2019**, *413*, 399–407. [CrossRef]
48. Bulushev, D.A.; Sobolev, V.I.; Pirutko, L.V.; Starostina, A.V.; Asanov, I.P.; Modin, E.; Chuvilin, A.L.; Gupta, N.; Okotrub, A.V.; Bulusheva, L.G. Hydrogen Production from Formic Acid over Au Catalysts Supported on Carbon: Comparison with Au Catalysts Supported on $SiO_2$ and $Al_2O_3$. *Catalysts* **2019**, *9*, 376. [CrossRef]